

Nuclei Detection Based on Single-point Labels

Valery Malyshau
Biomedical Image Analysis Department
United Institute of Informatics Problems of NAS of Belarus
Minsk, Belarus
malyshevalery@gmail.com

Abstract. Whole-slide image analysis is a long-lasting and laborious process. There are many ways of automatic analysis for histological images. The nuclei detection and classification is one of the most common and medically meaningful medical information-rich methods. However, sometimes the goal of nuclei detection is not to provide detailed information for the medical professionals but to be used for further aggregation. In such cases, nuclei segmentation exceeds requirements and takes extra resources during the data annotation. Keeping this in mind we optimized the existing state-of-art method for nuclei segmentation and classification to work with nucleus centers as input data. Combined with novel optimization technique and neural network activation function it resulted in the algorithm with has improved performance, easier training process and uses input data that is faster to produce.

Keywords: nuclei detection, neural networks, histology, cancer

I. INTRODUCTION

Whole-slide images (WSIs) are large images showing tissue morphology. Such images are the «gold standard» for cancer diagnosis. However large dimensions that can reach 100000px makes manual analysis an arduous task so histopathologists focus on important areas rather than analyzing every corner of an image [1]. Automatic analysis may reduce the workload but the outcome of algorithms must still be supervised by specialists. An ideal result of the automatic analysis would be the clinical outcome but intermediate results for example nuclei segmentation and classification produce significant insights into the data that can be used by specialists or other algorithms.

Nuclear detection is an essential task that arises during WSI analysis. It helps to quantify WSI for clinical and research reasons [2]. Regularly, detection is a union of segmentation and classification subtasks. In this work, we prioritize nuclear localization without specific boundary selection what helped us to build a more efficient algorithm that requires nuclei centers annotation. Such annotations require less time to obtain in comparison with conventional nuclei boundaries.

The nuclei detection problem is a regular object detection problem so a range of object detection methods were applied to it [3, 4] (F1 score equals 0.50 with classification and 0.94 for nuclei segmentation). However, relatively to WSIs and especially nuclei detection these methods do not show great performance comparing to other methods developed specifically for nuclei detection [5–7] (F1 for nuclei detection and classification falls in range of 0.7-0.86 depending on the method and dataset). There are several reasons for that i.e. large resolution of WSIs, data heterogeneity [8], many nuclei presented even on a small region of an image when current object detection methods work better with a relatively small number of various sized objects.

In this work, we use HoVer-Net [5] as a baseline for our model and evaluation procedure. This deep-learning model produces state-of-art results by combining U-Net shaped architecture with predicting vertical and horizontal maps for nuclei to split nearly located ones and then infer segmentation masks and classes for each presented nuclei.

As mentioned above WSI analysis is a laborious process, so is annotation and data preparation for deep learning. Therefore, we considered using points in nuclei centers as input data rather than complete boundaries around each nucleus. So the data preparation phase may be much faster and cheaper. In some works, instead of nuclei boundaries made by pathologists an algorithm was used to do that [9]. However, such methods can introduce an additional margin of error due to natural inaccuracies in machine learning algorithms. So we propose a method that works without considering nuclei segmentation. Even if in some cases segmentation is required [10], for example when nuclei shape features are the key for predicting an outcome, there are also cases when nuclei location and class would be enough [11] i.e. calculating amount of malignant nuclei on WSI. In addition to developing a deep-learning-based algorithm for processing point-annotated nuclei, we showed improved performance using novel advances among optimization procedures and activation functions for our deep-learning model and HoVer-Net.

The main contributions of this paper are listed below:

- Empirical evidence of performance improvement when novel optimization procedure and activation function are applied to the current state-of-art method for nuclei segmentation and classification.
- Efficient approach for nuclei detection using nucleus center maps scaled by recent advances in deep learning [12].

II. RELATED WORK

The main work which motivated us to work on optimizations and more effective use of medical annotations was the HoVer-Net deep learning architecture [5]. This model outperforms classical approaches from object detection like Mask-RCNN [13] or simplified detection procedures using segmentation networks such as U-Net [14] as well as their combinations [3]. Also, HoVer-Net shows surpassing accuracy in comparison with other deep learning models specified for nuclei detection [5–7]. Regarding the specifics of the deep-learning model, HoVer-Net can be seen as an improvement over typical U-Net with the residual and dense linkage between layers and several branches for classification and segmentation so an increased number of parameters and branches with specified purposes led to improved performance.

As we decided to work with raw nuclei labels in the center of nuclei we rejected models which goal was to create a mask for each nuclei or object in the case of general object detection algorithms. However, this work [15] proposes using predicted centers of objects as anchors for further segmentation by pyramid-like neural networks. Considering we worked with histology data with nuclei of the same size and images depicting the same magnification in borders of a single dataset we did not use feature pyramids and followed the HoVer-Net pattern with residual convolution with dense deconvolution in U-Net shape for predicting nuclei centers like in manner similar to the one described in [12].

III. MATERIALS

To provide relevant evidence that our method is as accurate as the original HoVer-Net we utilized the same subset of nuclei detection datasets. They included one classification dataset called CoNSeP [5] and several segmentation datasets which are CPM15 and CPM17 [16] TNBC [7] and Kumar [17]. We cut images from all datasets into square regions of the same size which we conveniently call tiles in this paper. Every tile was of size 256x256 pixels and they were extracted from original images with 128-pixel step. Detailed

information on datasets is shown in Table 1. Also, we used the union of CPM datasets for the sake of comparing them with the HoVer-Net paper. Datasets CPM15 and TNBC which included train test split so we could compare our results with ones provided for the original paper. In other cases, we created a random train test split which stayed the same during the experimental procedure. The same is applied for K-Fold evaluation in which case folds for experiments on one dataset using different methods were the same. Considering the small number of nuclei of miscellaneous class so the train test split affects the accuracy of this class a lot, we removed it from the CoNSeP dataset and in our iteration of HoVer-Net model training we kept this fact in mind.

TABLE I. DATASET INFORMATION

Dataset	N Images	N Nuclei	N tiles
CPM15	15	2 905	306
CPM17	32	7 570	337
Kumar	30	21 623	1470
TNBC	50	4 056	450
CoNSeP	41	24 319	2009

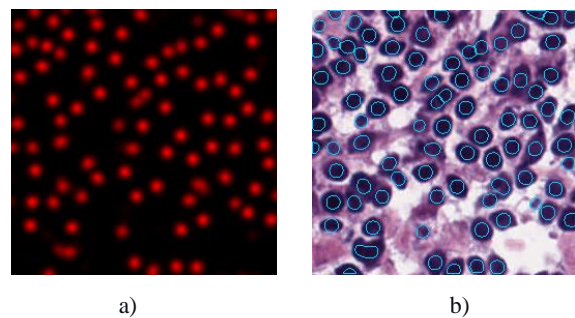


Fig. 1. Predicted a) nucleus centers map and b) resulting nucleus central areas

IV. METHOD

The algorithm for nuclei detection consists of two major parts. Firstly, we predict nuclei location using an adapted deep learning model. The deep learning model aims to predict nuclei locations as smoothed points in the nuclei centers. Ground truth data were single points blurred with a Gaussian kernel. Each channel on the resulting pseudo-image was the outcome for a single nuclei class. We trained the model with MSE loss.

Secondly, we ran a watershed algorithm on masks obtained from the deep learning model so the nuclei are split and the final result is obtained by taking the center of mass for each selected region. The example of nuclei center map and result of detection algorithm are presented in the Fig. 1.

Regarding the model, it was built with U-Net shaped architecture where the encoder is constructed from the residual blocks (2 convolutions with activations and residual link at the end) and the decoder

is made from dense blocks (3 convolutions with activations and acquired channels are attached to main features). The overview of the model is presented in Fig. 2. The whole algorithm can be viewed as a modification of a deep watershed [18] which uses a watershed algorithm to predict nuclei centers and separate them instead of regular segmentation masks.

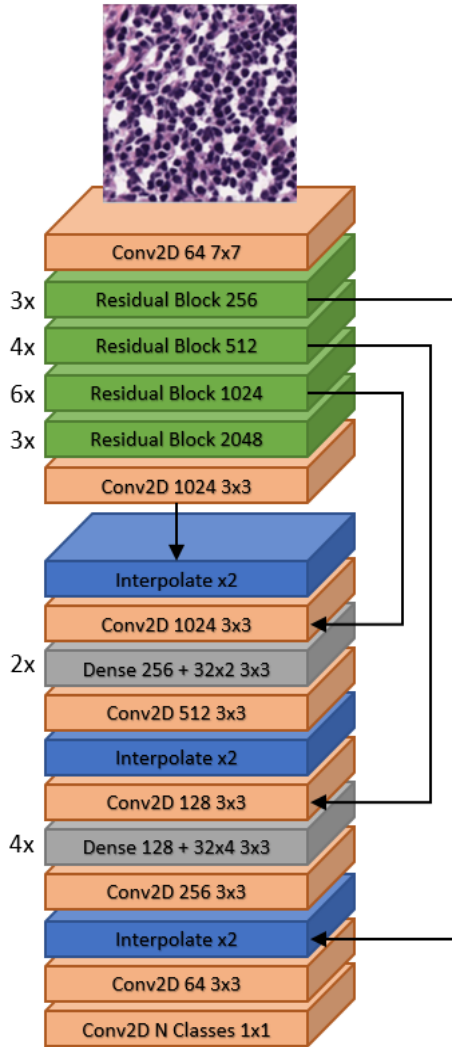


Fig. 2. Proposed Neural Network Architecture

Considering we used batch normalization between convolutional layers we applied novel optimization algorithm AdamP [19]. In addition, we changed conventional ReLU activation to Mish [20]. Together these two advancements improved the accuracy of our deep learning model and HoVer-Net trained for comparison in the same conditions.

V. RESULTS

To perform a thorough evaluation, we trained and tested both our algorithm and HoVer-Net with novel optimization technique and activation function using train test splits recommended by data providers. In several datasets, such splits were not provided so we created a random split and fixed it so the same data was used for training of both methods. On the other hand, we performed K-fold cross-validation with 5 folds to be able to obtain averaged scores considering relatively small sizes of datasets.

For evaluation, we chose F1 scores as our method do not work with segmentation masks so panoptic quality [21], Dice score and Aggregated Jaccard Index which composes detection and segmentation performance are not suitable in our case. Scores for comparison are presented in Table II.

Generally, both our model and HoVer-Net shows similar performance with some fracture of fluctuation.

VI. CONCLUSION

We showed that nuclei can be detected without the segmentation step which regularly is executed in either manual way or by another algorithm or deep learning model. Such an approach does not lose performance while being faster in training and inference. So if the desired result does not include nuclei segmentation it can be avoided while gaining benefits from the proposed model. Additionally, we tested novel optimization and activation function on histology data showing that their performance is higher than traditional methods when applied to histology nuclei detection data.

TABLE II. NEURAL NETWORKS TESTING SCORES

Method		Segmentation					CoNSeP (Classification)				
		CPM15	CPM17	All CPM	Kumar	TNBC	Epitheliu m	Inflammatory	Spindl e	Mean	Detectio n
HoVer-Net paper		-	0.854	0.774	0.770	0.743	0.635	0.631	0.566	0.565	0.748
K-Fold	HoVer-Net	0.882	0.892	0.896	0.864	0.878	0.766	0.781	0.694	0.747	0.815
	Our	0.868	0.895	0.893	0.875	0.879	0.727	0.775	0.658	0.720	0.793
Train/Test	HoVer-Net	-	0.870	-	0.829	-	0.699	0.677	0.616	0.664	0.772
	Our	-	0.862	-	0.812	-	0.713	0.716	0.614	0.681	0.773

REFERENCES

- [1] M. N. Gurcan, L. E. Boucheron, A. Can, A. Madabhushi, N. M. Rajpoot, and B. Yener, "Histopathological image analysis: a review," *IEEE reviews in biomedical engineering*, vol. 2, pp. 147–171, October 2009.
- [2] H. Irshad, A. Veillard, L. Roux, and D. Racoceanu, "Methods for nuclei detection, segmentation, and classification in digital histopathology: a review—current status and future potential," *IEEE reviews in biomedical engineering*, vol. 7, pp. 97–114, December 2013.
- [3] A. O. Vuola, S. U. Akram, and J. Kannala, "Mask-RCNN and U-net ensemble for nuclei segmentation," *IEEE 16th International Symposium on Biomedical Imaging (ISBI 2019)*, pp. 208–212, April 2019.
- [4] H. Narotamo, J. M. Sanches, and M. Silveira, "Combining deep learning with handcrafted features for cell nuclei segmentation," *42nd Annual International Conference of the IEEE Engineering in Medicine & Biology Society (EMBC)*, pp. 1428–1431, July 2020.
- [5] S. Graham, Q. D. Vu, S. E. A. Raza, A. Azam, Y. W. Tsang, J. T. Kwak, and N. Rajpoot, "Hover-net: simultaneous segmentation and classification of nuclei in multi-tissue histology images," *Medical Image Analysis*, vol. 58, pp. 101563., December 2019.
- [6] S. E. A. Raza, L. Cheung, M. Shaban, S. Graham, D. Epstein, S. Pelen-garis, M. Khan, and N. M. Rajpoot, "Micro-Net: a unified model for segmentation of various objects in microscopy images," *ArXiv e-prints*, p. arXiv:1804.08145, April 2018.
- [7] P. Naylor, M. La e, F. Reyat, and T. Walter, "Segmentation of nuclei in histopathology images by deep regression of the distance map," *IEEE Transactions on Medical Imaging*, vol. 38, pp. 448–459, August 2018.
- [8] Y. Xue, and N. Ray, "Cell detection in microscopy images with deep convolutional neural network and compressed sensing," *arXiv preprint*, p. arXiv:1708.03307, August 2017, unpublished.
- [9] L. Yang, R. P. Ghosh, J. M. Franklin, S. Chen, C. You, R. Narayan, et al., "NuSeT: a deep learning tool for reliably separating and analyzing crowded cells," *PLoS computational biology*, vol. 16, p. e1008193, September 2020.
- [10] Q. D. Vu, S. Graham, T. Kurc, M. N. N. To, M. Shaban, T. Qaiser, et al., "Methods for segmentation and classification of digital microscopy tissue images," *Frontiers in bioengineering and biotechnology*, vol. 7, p. 53, April 2019.
- [11] A. Kumar, and M. Prateek, "Localization of nuclei in breast cancer using whole slide imaging system supported by morphological features and shape formulas," *Cancer Management and Research*, vol. 12, p. 4573, 2020.
- [12] H. Höfener, A. Homeyer, N. Weiss, J. Molin, C. F. Lundström, H. K. Hahn, "Deep learning nuclei detection: a simple approach can deliver state-of-the-art results," *Computerized Medical Imaging and Graphics*, vol. 70, pp. 43–52, December 2018.
- [13] X. Xie, Y. Li, M. Zhang, and L. Shen, "Robust segmentation of nucleus in histopathology images via Mask R-CNN," *International MICCAI Brainlesion Workshop*, pp. 428–436, September 2018.
- [14] M. Z. Alom, C. Yakopcic, T. M. Taha, and V. K. Asari, "Nuclei segmentation with recurrent residual convolutional neural networks based U-Net (R2U-Net)," *NAECON 2018-IEEE National Aerospace and Electronics Conference*, pp. 228–233, July 2018.
- [15] H. Chen, and H. Zheng, "Object detection based on center point proposals," *Electronics*, vol. 9(12), p. 2075, December 2020.
- [16] Q. D. Vu, S. Graham, M. N. N. To, M. Shaban, T. Qaiser, N. A. Koozbanani, S. A. Khurram, et al., "Methods for segmentation and classification of digital microscopy tissue images," *Frontiers in bioengineering and biotechnology*, vol. 7, pp. 53., April 2019.
- [17] N. Kumar, R. Verma, S. Sharma, S. Bhargava, A. Vahadane, and A. Sethi, "A dataset and a technique for generalized nuclear segmentation for computational pathology," *IEEE Transactions on Medical Imaging*, vol. 36, pp. 1550–1560, July 2017.
- [18] M. Bai, R. Urtasun, "Deep watershed transform for instance segmentation," *Proceedings of the IEEE Conference on Computer Vision and Pattern Recognition*, pp. 5221–5229, 2017.
- [19] B. Heo, S. Chun, S. J. Oh, D. Han, S. Yun, G. Kim, G., et al., "AdamP: slowing down the slowdown for momentum optimizers on scale-invariant weights," *Proceedings of the International Conference on Learning Representations (ICLR)*, pp. 3–7, May 2021.
- [20] D. Misra, "Mish: A self regularized non-monotonic neural activation function," *arXiv preprint*, p. arXiv:1908.08681, October 2019, unpublished.
- [21] A. Kirillov, K. He, R. Girshick, C. Rother, and P. Dollár, "Panoptic segmentation," *Proceedings of the IEEE/CVF Conference on Computer Vision and Pattern Recognition*, pp. 9404–9413, 2019.